Vol 15 No 9, September 2006
1009-1963/2006/15(09)/2108-06

Chinese Physics

© 2006 Chin. Phys. Soc.
and IOP Publishing Ltd

Calculation of phonon spectrum for noble metals by modified analytic embedded atom method (MAEAM)*

Zhang Xiao-Jun(张晓军)[a], Zhang Jian-Min(张建民)[a]†, and Xu Ke-Wei(徐可为)[b]

[a] *College of Physics and Information Technology, Shaanxi Normal University, Xi'an 710062, China*

[b] *State Key Laboratory for Mechanical Behavior of Materials, Xi'an Jiaotong University, Xi'an 710049, China*

(Received 25 January 2006; revised manuscript received 9 May 2006)

In the harmonic approximation, the atomic force constants are derived and the phonon dispersion curves along four major symmetry directions [00ζ], [0ζζ], [ζζζ] and [0ζ1] (or Δ, Σ, Λ and Z in group-theory notation) are calculated for four noble metals Cu, Ag, Au and Pt by combining the modified analytic embedded atom method (MAEAM) with the theory of lattice dynamics. A good agreement between calculations and measurements, especially for lower frequencies, shows that the MAEAM provides a reasonable description of lattice dynamics in noble metals.

Keywords: noble metals, lattice dynamics, MAEAM
PACC: 7155D, 6320, 6300

1. Introduction

A detailed knowledge of the dispersion relations arising from lattice vibrations in metals is important for studying accurately various thermodynamic quantities such as lattice molar heat capacity, density of states, thermal expansion coefficient, Debye temperature and electron–phonon effects.[1−6] The phonon dispersions of the transition metals have been studied experimentally over the past few years. A number of experimental techniques, thermal neutron inelastic scattering for example, have been conducted to measure the phonon dispersion curves of several face-centred cubic (FCC) metals.[7] In principle, detailed phonon dispersion curves can be determined and then analysed to yield information about the interatomic forces. The analyses are made in terms of the lattice dynamics theory which employs the harmonic approximation and yields a set of interatomic force constants of as many nearest neighbours as they are required to fit the data. One might expect that such a force constant model can reproduces the experimental dispersion curves.

Two-body central potential model has long been used to describe the metallic bondings. Although it is simple, the utilization is limited by the breakdown in the two-body approximation.[8] The deficiency may be remedied by using a many-body potential model. In contrast to central force potentials in which only the potential energy of a system of particles is considered, one of the many-body models developed by Dow and Baskes,[9,10] embedded atom method (EAM), presents the energy of an atom in a system as a sum of the electrostatic interactions between this atom and each of its adjacent atoms and the energy required to embed the atom to the local electron density created by its adjacent atoms. However, in the EAM and the analytic embedded atom method (AEAM) extended by Johnson,[11−14] the bond angles are not considered in the expression of electron density. In order to reflect exactly the interaction between atoms, Zhang *et al*[15,16] developed a modified analytic embedded atom method (MAEAM), by adding a modified term $M(P)$ to the total energy expression for the AEAM to express the difference between the accrual total energy of a system of atoms and that calculated from the AEAM using a linear superposition of spherical atomic electron densities. The model was successful in calculating the interface energy,[17−19] the grain boundary energy[20−22] for FCC metals, the vacancy diffusion

*Project supported by the State Key Program of Basic Research of China (Grant No 2004CB619302) and the National Natural Science Foundation of China (Grant No 50271038).

†E-mail: jianm_zhang@yahoo.com

mechanism for all bcc transition metals.[16]

In this paper, the lattice dynamical matrix is derived from the MAEAM, and then the phonon dispersion curves are calculated for four noble metals Cu, Ag, Au and Pt with wave vectors along four major symmetry directions [00ζ], [0$\zeta\zeta$], [$\zeta\zeta\zeta$] and [0ζ1], or Δ, Σ, Λ and Z in group-theory notation. We can see that the MAEAM is able to predict bulk phonon modes in excellent agreement with experiment. The agreement shows that the modified analytic embedded atom method provides a reasonable description of transition metal lattice dynamics.

2. Modified analytical embedded atom method

In the MAEAM, the total energy of a system of atoms $E_{\rm t}$ is expressed as[23−25]

$$E_{\rm t} = \sum_i F(\rho_i) + \frac{1}{2}\sum_i \sum_{j\neq i} \phi(r_{ij}) + \sum_i M(P_i), \quad (1)$$

$$\rho_i = \sum_{j\neq i} f\left(r_{ij}\right), \quad (2)$$

$$P_i = \sum_{j\neq i} f^2\left(r_{ij}\right), \quad (3)$$

where $F(\rho_i)$ is the energy required to embed an atom on site i with electron density ρ_i, which is given by a linear superposition of the spherical averaged atomic electron density of other atoms $f(r_{ij})$, r_{ij} is the separation between atom j and atom i, $\phi(r_{ij})$ is the interaction potential between atom i and atom j, and $M(P_i)$ is the modified term that describes the energy change due to the non-spherical distribution of electrons (P_i) and the deviation from the linear superposition of atomic electronic densities. The embedding function $F(\rho_i)$, pair potential $\phi(r_{ij})$, modified term $M(P_i)$ and atomic electron density $f(r_{ij})$ take the following forms:[23−25]

$$F(\rho_i) = -F_0\left[1 - n\ln\left(\rho_i/\rho_{\rm e}\right)\right]\left(\rho_i/\rho_{\rm e}\right)^n, \quad (4)$$

$$\begin{aligned}\phi\left(r_{ij}\right) =& k_0 + k_1\left(r_{ij}/r_{1{\rm e}}\right) + k_2\left(r_{ij}/r_{1{\rm e}}\right)^2 \\ &+ k_3\left(r_{ij}/r_{1{\rm e}}\right)^6 + k_4\left(r_{ij}/r_{1{\rm e}}\right)^{-12} \\ &+ k_5\left(r_{ij}/r_{1{\rm e}}\right)^{-1}, \end{aligned} \quad (5)$$

$$M\left(P_i\right) = \alpha\left\{1 - \exp\left[-\left(\ln\left|P_i/P_{\rm e}\right|\right)^2\right]\right\}, \quad (6)$$

$$f(r_{ij}) = f_{\rm e}(r_{1{\rm e}}/r_{ij})^6, \quad (7)$$

where the subscript e indicates equilibrium state and $r_{1{\rm e}}$ is the distance from the most adjacent atom in equilibrium. The cut-off distance of interaction potential for FCC metals $r_{\rm ce}$, where the pair potential and its slope are zero, lies in the distance between the fifth and the sixth neighbours, that is $r_{\rm ce} = r_{5{\rm e}} + k_{\rm ce}(r_{6{\rm e}} - r_{5{\rm e}})$, in which $k_{\rm ce}$ is a model parameter that is to be fitted. F_0 and $f_{\rm e}$ can be calculated from[24]

$$F_0 = E_{\rm c} - E_{1{\rm v}}, \quad (8)$$

$$f_{\rm e} = \sqrt{E_{\rm c}}/\Omega, \quad (9)$$

where $E_{\rm c}$ is the cohesion energy, $E_{1{\rm v}}$ is the mono-vacancy formation energy and $\Omega = a^3/4$ is the atomic volume in FCC metals.

The remaining model parameters can be calculated from the physical parameters,[25] the lattice constant a, cohesive energy $E_{\rm c}$, mono-vacancy formation energy $E_{1{\rm v}}$ and elastic constants C_{11}, C_{12} and C_{44}. The physical parameters used in this paper and the calculated model parameters for the noble metals are listed in Tables 1 and 2, respectively.

Table 1. The input physical parameters for noble metals.

metal	a/nm	$E_{\rm c}$/eV	$E_{1{\rm v}}$/eV	C_{11}/GPa	C_{12}/GPa	C_{44}/GPa
Cu	0.36147	3.49	1.17	169.0	122.0	75.3
Ag	0.40857	2.95	1.10	123.0	92.0	45.3
Au	0.40788	3.81	0.90	190.0	161.0	42.3
Pt	0.39239	5.84	1.20	347.0	251.0	76.5

Table 2. The calculated model parameters for noble metals.

parameter	Cu	Ag	Au	Pt
n	0.60	0.82	0.94	0.980
$k_{\rm ce}$	0.3	0.3	0.3	0.3
F_0/eV	2.32	1.85	2.91	4.64
α/eV	0.00316257	–0.0001666	0.0048	0.0051
k_0/eV	1.499487	0.2821774	1.1566	–0.5866
k_1/eV	–0.650171	0.1474579	–0.4510	1.4604
k_2/eV	0.097645	–0.0803378	0.0541	–0.5196
k_3/eV	–0.000056	0.000303516	–0.00006	0.0020
k_4/eV	0.098837	0.084663779	0.0803	0.134
k_5/eV	–1.178326	–0.55494136	–0.9523	–0.7491

3. Lattice dynamics

The general theory of lattice dynamics has already been described in literature,[26,27] and the most relevant results are presented here. For the Bravais crystals, the frequencies ω and the polarization vectors ξ of the normal modes of the crystal vibration satisfy the following equation in the harmonic approximation:

$$M\omega^2\xi_\alpha = \sum_\beta \xi_\beta D_{\alpha\beta}\left(\boldsymbol{q}\right), \tag{10}$$

where α, β=1, 2, 3 refer to Cartesian coordinates, M is the mass of the atom, and the $D_{\alpha\beta}\left(\boldsymbol{q}\right)$, the elements of the dynamical matrix, are given by

$$D_{\alpha\beta}\left(\boldsymbol{q}\right) = \sum_j \Phi_{\alpha\beta}\left(i,j\right) \mathrm{e}^{\mathrm{i}\boldsymbol{q}\cdot\left[\boldsymbol{r}(j)-\boldsymbol{r}(i)\right]}, \tag{11}$$

where $\boldsymbol{q}$ is the wave vector, j runs over all atoms of the entire crystal, $\boldsymbol{r}\left(i\right)$ and $\boldsymbol{r}\left(j\right)$ are respectively the vector coordinates of the ith and jth atoms at their equilibrium positions with respect to the atom at the origin. The $\Phi_{\alpha\beta}\left(i,j\right)$, the atomic force constants, which represent the force acting on the atom at position $\boldsymbol{r}\left(i\right)$ in the direction α when the atom at position $\boldsymbol{r}\left(j\right)$ is given a unit displacement in the direction β, can be calculated by evaluating the second derivative of the total energy of a system of atoms $E_{\rm t}$ with respect to atom coordinates

$$\Phi_{\alpha\beta}\left(i,j\right) = \frac{\partial^2 E_{\rm t}}{\partial r_\alpha\left(i\right)\partial r_\beta\left(j\right)}. \tag{12}$$

Inserting Eq.(1) into Eq.(12), we can obtain

$$\Phi_{\alpha\beta}\left(i,j\right) = \Phi^{(1)}_{\alpha\beta}\left(i,j\right) + \Phi^{(2)}_{\alpha\beta}\left(i,j\right) + \Phi^{(3)}_{\alpha\beta}\left(i,j\right), \tag{13}$$

where $\Phi^{(1)}_{\alpha\beta}\left(i,j\right)$, $\Phi^{(2)}_{\alpha\beta}\left(i,j\right)$ and $\Phi^{(3)}_{\alpha\beta}\left(i,j\right)$ are the atomic force constants contributed by the two-body potential, embedding function and modify term respectively, and they are respectively in the following forms:

$$\Phi^{(1)}_{\alpha\beta}\left(i,j\right) = -\frac{r_{ij\alpha}r_{ij\beta}}{r_{ij}^2}\left[\phi''\left(r_{ij}\right) - \frac{\phi'\left(r_{ij}\right)}{r_{ij}}\right] - \delta_{\alpha\beta}\frac{\phi'\left(r_{ij}\right)}{r_{ij}}, \tag{14}$$

$$\begin{aligned}\Phi^{(2)}_{\alpha\beta}(i,j) = &-\left[F'\left(\rho_i\right)f''\left(r_{ij}\right) + F'\left(\rho_j\right)f''\left(r_{ij}\right)\right]\frac{r_{ij\alpha}r_{ij\beta}}{r_{ij}^2}\\ &- f'\left(r_{ij}\right)\left[F'\left(\rho_i\right) + F'\left(\rho_j\right)\right]\times\left(\frac{\delta_{\alpha\beta}}{r_{ij}} - \frac{r_{ij\alpha}r_{ij\beta}}{r_{ij}^3}\right)\\ &- F''\left(\rho_i\right)f'\left(r_{ij}\right)\frac{r_{ij\beta}}{r_{ij}}\sum_{m\neq i} f'\left(r_{im}\right)\frac{r_{im\alpha}}{r_{im}}\\ &- F''\left(\rho_j\right)f'\left(r_{ij}\right)\frac{r_{ij\alpha}}{r_{ij}}\sum_{m\neq j} f'\left(r_{jm}\right)\frac{r_{jm\beta}}{r_{jm}}\\ &+ \sum_{m\neq i,j} F''\left(\rho_m\right)f'\left(r_{im}\right)f'\left(r_{jm}\right)\frac{r_{jm\beta}}{r_{jm}}\frac{r_{im\alpha}}{r_{im}},\end{aligned} \tag{15}$$

$$\begin{aligned}\Phi^{(3)}_{\alpha\beta}(i,j) =& -2\left[M'(P_i)+M'(P_j)\right]\times\left[f(r_{ij})f''(r_{ij})+f'(r_{ij})^2\right]\frac{r_{ij\alpha}r_{ij\beta}}{r_{ij}^2}\\ &-2\left[M'(P_i)+M'(P_j)\right]\frac{f(r_{ij})f'(r_{ij})}{r_{ij}}\left(\delta_{\alpha\beta}-\frac{r_{ij\alpha}r_{ij\beta}}{r_{ij}^2}\right)\\ &-4M''(P_i)f(r_{ij})f'(r_{ij})\frac{r_{ij\beta}}{r_{ij}}\sum_{m\neq i}f(r_{im})f'(r_{im})\frac{r_{im\alpha}}{r_{im}}\\ &+4M''(P_j)f(r_{ij})f'(r_{ij})\frac{r_{ij\alpha}}{r_{ij}}\sum_{m\neq j}f(r_{jm})f'(r_{jm})\frac{r_{jm\beta}}{r_{jm}}\\ &-4\sum_{m\neq i,j}M''(P_m)f(r_{jm})f'(r_{jm})\frac{r_{jm\beta}}{r_{jm}}f(r_{im})f'(r_{im})\frac{r_{im\alpha}}{r_{im}},\end{aligned}\tag{16}$$

in which $r_{ij}=|\boldsymbol{r}(j)-\boldsymbol{r}(i)|$ is the distance between atom i and atom j, prime and double-prime symbols represent the first and second derivatives respectively, $\delta_{\alpha\beta}$=1 if $\alpha=\beta$, and is zero otherwise.

The condition for Eq.(10) to have solutions different from zero is that the secular determinant (17) is zero

$$\det\left|D_{\alpha\beta}(\boldsymbol{q})-M\omega^2\delta_{\alpha\beta}\right|=0.\tag{17}$$

Then the frequencies ω can be obtained by solving Eq.(17) with Eqs. (11), (13)–(16).

4. Results and discussion

A computational cell surrounded by a mantle of atoms is used in computation. The computational cell is a $6a\times6a\times6a$ crystal with 1099 atoms, in which a is a lattice constant of the metal considered. The mantle ensures that each atom in the computational cell has a complete set of adjacent atoms within the range of the interatomic potential. In the calculation of the pair potential contributions to the atomic force constants of atom i, in principle, the sum of the contributions from all other atoms j in the crystal should be required. In practice, however, only the atom j, which is separated from atom i by a distance shorter than the cut-off distance of interaction potential $r_{\rm ce}$ (that is $r_{ij}<r_{\rm ce}$), needs to be considered. Analogously, in the calculation of the embedding function and modified term contributions to the atomic force constants of atom i, we take into account only those atoms located at distances less than $r_{\rm cf}$ from atom i. In this paper, the atomic electronic density $f(r_{ij})$ is truncated at a specific cutoff distance

$$r_{\rm cf}=r_{6\rm e}+k_{\rm cf}(r_{7\rm e}-r_{6\rm e}),\tag{18}$$

in which $k_{\rm cf}=0.75$ is the model parameter. When the separation r_{ij} between atoms i and j is larger than $r_{\rm cf}$ (that is $r_{ij}>r_{\rm cf}$), both the $f(r_{ij})$ and $f'(r_{ij})$ are equal to zero. As shown schematically in Fig.1(a), if $r_{ij}>2r_{\rm cf}$, the atomic force constants $\Phi^{(2)}_{\alpha\beta}(i,j)$ and $\Phi^{(3)}_{\alpha\beta}(i,j)$ are equal to zero. While $r_{\rm cf}<r_{ij}<2r_{\rm cf}$ in Fig.1(b), the last terms on the right-hand sides of Eqs.(15) and (16) are not equal to zero because the atoms i and j interact indirectly through the other atoms m which are at distances less than $r_{\rm cf}$ from both atoms i and j. If $r_{ij}<r_{\rm cf}$ in Fig.1(c), the atoms i and j interact directly as well as indirectly through the other atoms m, then the five terms of Eqs.(15) and (16) must be evaluated respectively.

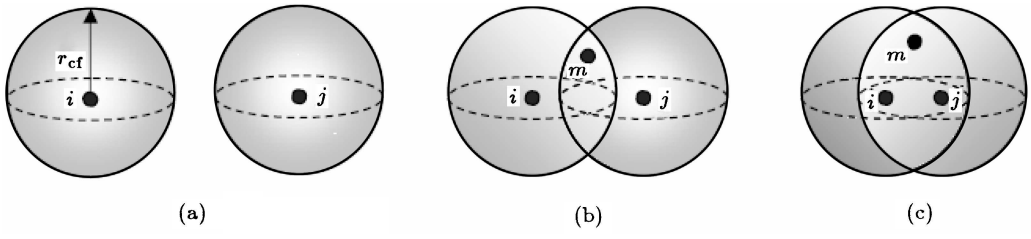


Fig.1. (a) $r_{ij}>2r_{\rm cf}$, atoms i and j do not interact with each other, (b) $r_{\rm cf}<r_{ij}<2r_{\rm cf}$, atoms i and j do not directly interact with each other but indirectly through an atom m, (c) $r_{ij}<r_{\rm cf}$, atoms i and j directly as well as indirectly interact with each other through an atom m.

The dispersion curves calculated by combining the MAEAM with the theory of lattice dynamics along four principal symmetry directions are shown in Figs.2, 3, 4 and 5 for Cu, Au, Ag and Pt respectively together with their experimental values for comparison. Along both [00ζ] and [ζζζ] directions, two transverse modes T_1 and T_2 merge into a dispersion curve due to four- and six-fold rotation symmetries respectively about these two directions.[28,29] The following special points can be obtained from these figures. Firstly, the shapes of calculated dispersion curves are generally consistent with experimental results for the four noble metals along the four directions considered. This shows that the MAEAM provides a physically reasonable description of the vibrational excitations of a noble metal. Secondly, a good agreement of the calculations with experimental results at lower wave vectors q (or lower frequencies ω) rather than at the first Brillouin zone boundaries for the longitudinal mode L at $q = (001)\,2\pi/a$, the transverse mode T_2 at $q = (011)\,2\pi/a$ and the longitudinal mode L at $q = \left(\frac{1}{2}\frac{1}{2}\frac{1}{2}\right) 2\pi/a$ for all metals, may result from the fact that at longer wave limitation the crystal can be suitably treated as a continuum and the elastic constants, used as fitting modal parameters, are the reasonable parameters describing small deformation of a continuum. Thirdly, one of causes for the vibrational frequencies along the same symmetry direction to successively decrease for Cu, Ag, Pt and Au is the successive increase in mass for Cu, Ag, Pt and Au.

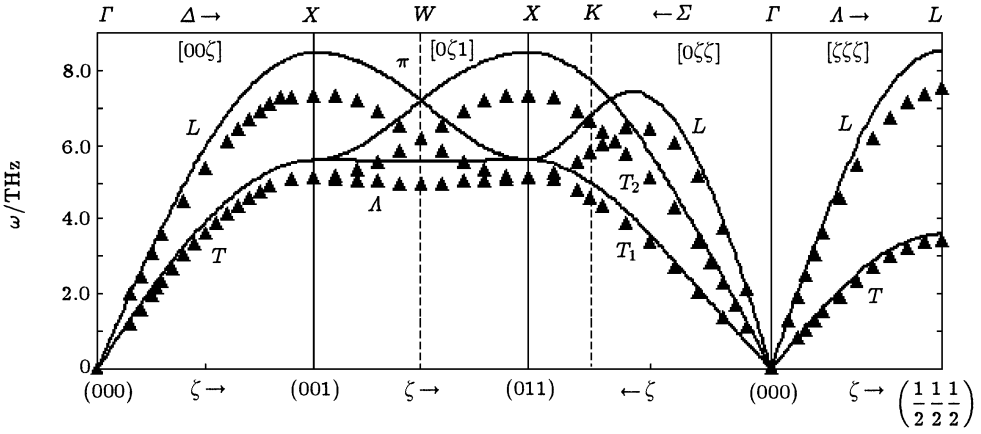


Fig.2. Calculated phonon dispersion curves for Cu with the triangles denoting the experimental data by Svensson *et al*[26].

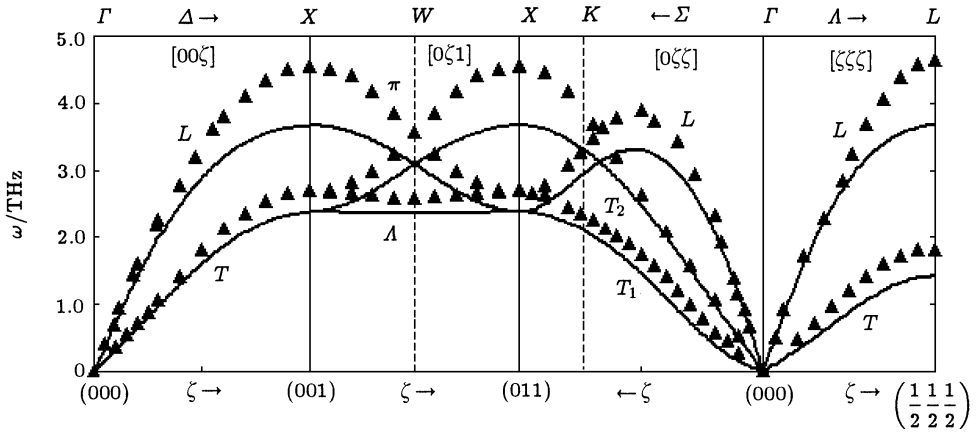


Fig.3. Calculated phonon dispersion curves for Au with the triangles denoting the experimental data by Lynn *et al*[30].

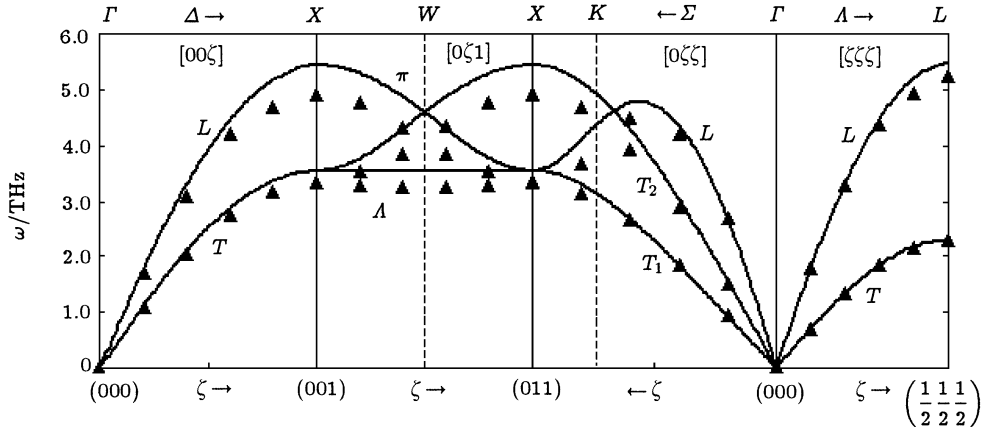


Fig.4. Calculated phonon dispersion curves for Ag with the triangles representing the experimental data by Kamitakahara *et al*[31].

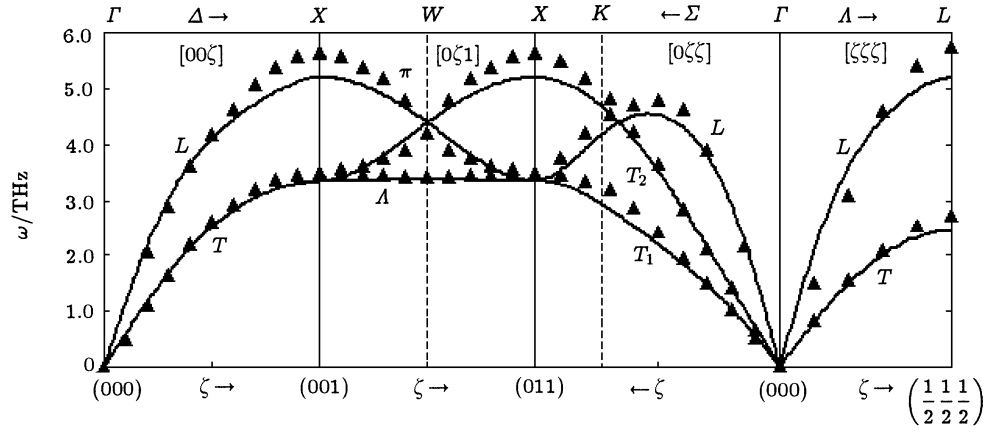


Fig.5. Calculated phonon dispersion curves for Pt with the triangles referring to the experimental data by Dutton *et al*[32].

References

[1] Gilat G and Nicklow R M 1966 *Phys. Rev.* **143** 487
[2] Atake T, Abe R, Honda K and Kawaji H 2000 *J. Phys. Chem. Solids* **611** 373
[3] An Z, Li A J, Liu Y and Li Y C 2000 *Chin. Phys.* **9** 37
[4] Yu C F, Chen B and He G Z 1994 *Acta Phys. Sin.* **43** 839 (in Chinese)
[5] Liang X X and Shi L 2004 *Chin. Phys.* **13** 71
[6] Zhong H Q 2004 *Acta Phys. Sin.* **53** 1162 (in Chinese)
[7] Birgeneau R J, Cordes J, Dolling G and Woods A D B 1964 *Phys. Rev.* A **136** 1359
[8] Nelson J S, Sowa E C and Daw M S 1988 *Phys. Rev. Lett.* **61** 1977
[9] Dow M S and Baskes M I 1983 *Phys. Rev. Lett.* **50** 1285
[10] Dow M S and Baskes M I 1984 *Phys. Rev.* B **29** 6443
[11] Johnson R A 1988 *Phys. Rev.* B **37** 3924
[12] Johnson R A 1989 *Phys. Rev.* B **39** 12554
[13] Johnson R A 1996 *Surf. Sci.* **355** 241
[14] Johnson R A 1990 *Phys. Rev.* B **41** 9717
[15] Ouyang Y F, Zhang B W, Liao S Z and Jin Z P 1996 *Z. Phys.* B **101** 161
[16] Zhang B W, Ouyang Y F, Liao S Z and Jin Z P 1999 *Phys.* B **262** 218
[17] Ma F, Zhang J M and Xu K W 2004 *Surf. Interface Anal.* **36** 355
[18] Zhang J M, Xin H and Xu K W 2005 *Appl. Surf. Sci.* **246** 14
[19] Xin H, Zhang J M, Wei X M and Xu K W 2005 *Surf. Interface Anal.* **37** 608
[20] Zhang J M, Wei X M and Xin H 2004 *Surf. Interface Anal.* **36** 1500
[21] Zhang J M, Wei X M, Xin H and Xu K W 2005 *Chin. Phys.* **14** 1015
[22] Zhang J M, Wei X M and Xin H 2005 *Appl. Surf. Sci.* **243** 1
[23] Hu W Y, Zhang B W, Shu X L and Huang B Y 1999 *J. Alloys Comp.* **287** 159
[24] Hu W Y, Shu X L and Zhang B W 2002 *Comput. Mater. Sci.* **23** 175
[25] Fang F, Shu X L, Deng H Q, Hu W Y and Zhu M 2003 *Mater. Sci. Engin.* A **355** 357
[26] Svensson E C, Vrockhouse B M and Rowe J M 1967 *Phys. Rev.* **155** 619
[27] Woods A D B, Brockhouse B N, March R H and Stewart A T 1962 *Phys. Rev.* **128** 1112
[28] Zhang J M and Xu K W 2001 *Appl. Surf. Sci.* **180** 1
[29] Zhang J M, Zhang Y and Xu K W 2005 *Phys.* B **368** 215
[30] Lynn J W, Smith H G and Nicklw R M 1973 *Phys. Rev.* B **8** 3493
[31] Kamitakahara W A and Brockhouse B N 1969 *Phys. Lett.* A **29** 639
[32] Dutton D H, Brockhouse B N and Miller A P 1972 *Can. J. Phys.* **50** 2915